DMD#18853

CYP2D6 mediated metabolism of a novel ACAT inihibitor, pactimibe, and its unique plasma metabolite, R-125528

Masakatsu Kotsuma, Taro Tokui, Tomoko Ishizuka-Ozeki, Tomoyo Honda, Haruo Iwabuchi, Takahiro Murai, Toshihiko Ikeda, and Hideo Saji

Drug Metabolism and Pharmacokinetics Research Laboratories, Daiichi-Sankyo Co., Ltd., Tokyo, Japan (M.K., T.T., T.I.-O., T.H., H.I., T.M., and T.I.); and Department of Patho-Functional Bioanalysis, Graduate School of Pharmaceutical Sciences, Kyoto University, Kyoto, Japan (H.S.)

Running title: CYP2D6 mediated metabolism of pactimibe and R-125528

Corresponding Author: Masakatsu Kotsuma

Address:

DAIICHISANKYO CO., LTD.

1-2-58, Hiromachi, Shinagawa-ku, Tokyo 140-8710, Japan

Phone: +81-2-3492-3131, Fax: +81-3-5436-8567

E-mail: kotsuma.masakatsu.gu@daiichisankyo.co.jp

Text Pages: 22

Abstract: 237 words

Introduction: 533 words

Discussion: 1138 words

Tables: 3

Figures: 4

References: 34

Abbreviations: ACAT, Acyl coenzyme A:cholesterol acyltransferase; P450, cytochrome P450; HPLC, high performance liquid chromatography; LC-MS/MS, liquid chromatography/tandem mass spectrometry; CLint, intrinsic clearance; AUC^{EM}, area under the plasma concentration time curve in CYP2D6 extensive metabolizer; AUC^{PM}, area under the plasma concentration time curve in CYP2D6 poor metabolizer

Abstract

Pactimibe sulfate is a novel ACAT inhibitor. We conducted metabolic studies of pactimibe and its plasma metabolite, R-125528. Pactimibe had multiple metabolic pathways including indolin oxidation to form R-125528, ω-1 oxidation, N-dealkylation and glucuronidation. Among them, the indolin oxidation and the ω-1 oxidation were dominant and were mainly catalyzed by CYP3A4 and CYP2D6, respectively. The CLint values for these pathways in human hepatic microsomes were 0.63 and 0.76 μl/min/mg-protein, respectively. On the other hand, the metabolic reaction for R-125528 was restricted. It was demonstrated that ω-1 oxidation was the only pathway that could eliminate R-125528 from the systemic circulation. To our surprise, only CYP2D6 expressing microsomes could catalyze the reaction, and ω-1 oxidation was strongly correlated with the CYP2D6 marker reaction, dextromethorphan O-demethylation (r^2=0.90) in human hepatic microsomes. Although R-125528 is an atypical substrate for CYP2D6 due to its acidity, the Km value was 1.8 μM for the reaction in human hepatic microsomes and the CLint value was as high as 75.0 μl/min/mg-protein. These results suggested that the systemic clearance of R-125528 was highly dependent on CYP2D6 activity, and that several studies with CYP2D6 including drug-drug interaction and polymorphism sensitivity should be conducted during development from the viewpoint of metabolite safety assessment. The finding that R-125528, an acidic compound devoid of basic nitrogen, was a good substrate for CYP2D6 raised a question about previously reported CYP2D6 models based on a critical electrostatic interaction with Asp[301] and/or Glu[216].

Introduction

Pactimibe sulfate [7-(2,2-dimethylpropanamido)-4,6-dimethyl-1-octylindolin-5-yl] acetic acid hemisulfate (formerly named CS-505, Figure 1) is a novel ACAT inhibitor used to treat hypercholesterolemia and atherosclerotic diseases (Nissen et al., 2006; Kitayama et al., 2006a, 2006b, 2006c). A number of ACAT inhibitors have been evaluated by several investigators. However, because of poor pharmacokinetics (Peck et al., 1995), adverse effects such as adrenal toxicity (Matsuo et al., 1996; Reindel et al., 1994; Vernetti et al., 1993), diarrhea (Kashiwa et al., 1997) and hepatotoxicity (Ishi et al., 1994; Nakaya et al., 1994), and elusive efficacies in humans (Hainer et al., 1994; Harris et al., 1990; Tardif et al., 2004), none of these compounds have so far succeeded in clinical development.

Pactimibe sulfate was selected as a clinical development candidate showing good oral absorbability and potent pharmacological effects in apolipoprotein E-deficient mice (Terasaka et al., 2007) and Watanabe heritable hyperlipidemic rabbits (Kitayama et al., 2006b), and without showing significant adrenal toxicity even in dogs, the most sensitive animal species

Pactimibe is a weak acidic compound and has several metabolic pathways including oxidation at the indolin ring, ω-1 oxidation at the octyl chain, N-dealkylation and glucuronidation on the carboxylic acid. Kinetic studies using human liver microsomes revealed that indolin ring oxidation (formation of R-125528) and ω-1 oxidation (formation of M-1) were equally dominant and that glucuronidation and N-dealkylation were minor. In addition, none of the metabolites were estimated to be

4

pharmacologically active *in vitro*.

In vivo biotransformation studies in animals demonstrated that only pactimibe and R-125528, the oxidized form of the indolin ring in pactimibe, appeared in the plasma and that none of the other metabolites were observed. After oral administration of pactimibe sulfate at a dose of 1 mg/kg to rats, dogs, and monkeys, $AUC_{R-125528}/AUC_{pactimibe}$ ratios were calculated to be 3, 14, and 55%, respectively. On the other hand, pactimibe and R-125528 were not detected in the urine or bile but were excreted into the bile as further metabolized forms.

R-125528 is quite a unique metabolite which has higher lipophilicity than the parent compound does. In general, biotransformation converts nonpolar, lipophilic pharmacologically active drug molecules into polar, inactive or nontoxic metabolites that are readily eliminated from the body (Venkatakrishnan et al., 2001). Interestingly, however, an oxidation from the indolin ring to indole ring leads pactimibe (LogP: 4.68) into more lipophilic R-125528 (LogP: 5.83). Then, R-125528 has to be further metabolized to be eliminated from systemic circulation, forcing us to conduct extensive biotransformation studies of R-125528.

To our surprise, metabolic studies using human liver microsomes and human P450 expressing systems revealed that R-125528 was sorely metabolized by CYP2D6, even though R-125528 is an acidic compound with a carboxyl group and without basic nitrogen in the structure, suggesting it is an atypical CYP2D6 substrate. When the drug has only a single elimination pathway mediated by a polymorphic enzyme such as CYP2D6, its AUC could drastically increase in patients who lack the enzyme genetically

and/or who take concomitant medication which inhibit the enzyme activity, leading to enhanced side effects.

In this study, we conducted metabolic studies of pactimibe and its plasma metabolite, R-125528, and then discussed the clinical outcomes of drug-drug interactions and genetic polymorphism on the metabolic enzymes responsible for the clearance.

Methods

Test substances and reagents

Pactimibe sulfate [7-(2,2-dimethylpropanamido)-4,6-dimethyl-1-octylindolin-5-yl] acetic acid hemisulfate and R-125528 were synthesized at the Process Development Laboratories, Sankyo Co., Ltd. (Tokyo, Japan). ^{14}C-pactimibe was synthesized at Amersham Pharmacia Biotech Limited (Tokyo, Japan). M-1, d_6-M-1 and M-2 were synthesized at Chemtec Labo., Inc. (Tokyo, Japan). The chemical structure of pactimibe sulfate is shown in Figure 1. NADP, glucose-6-phosphate and glucose-6-phosphate dehydrogenase were purchased from Sigma-Aldrich (St. Louis, MO). $MgCl_2 \cdot 6H_2O$ was purchased from Wako Pure Chemical Industries, Ltd (Osaka, Japan). Acetonitrile of HPLC grade and 1N HCl of volumetric analysis grade were purchased from Wako Pure Chemical Industries, Ltd (Osaka, Japan). Other reagents and solvents were of analytical grade and used without further purification.

In vitro metabolism study

Microsomes expressing human P450 isoforms: Human lymphoblast microsomes expressing human P450 isoforms, CYP1A1 (Lot No. 36), CYP1A2 (Lot No. 69), CYP1B1 (Lot No. 9), CYP2A6 (Lot No. 41), CYP2B6 (Lot No. 48), CYP2C8 (Lot No. 31), CYP2C9 (Lot No. 44), CYP2C19 (Lot No. 38), CYP2D6 (Lot No. 43), CYP2E1 (Lot No. 41) , CYP3A4(Lot No. 73) , CYP4A11 (Lot No. 8) and control microsomes (Lot No. 28) were purchased from Gentest (Woburn, MA). Microsomes were stored at -80°C until use.

Human liver microsomes: Human liver microsomes (mixed pool, 15) were purchased from In Vitro Technologies, Inc. (Baltimore, MD) and used to determine enzyme kinetic parameters. A Reaction Phenotyping Kit (Version 5) including 16 individual human liver microsomes was purchased from Xenotech, LLC (Kansas City, KS). The microsomes had been characterized with respect to the following enzyme activities: 7-ethoxyresorufin O-dealkylation (CYP1A2), coumarin 7-hydroxylation (CYP2A6), S-mephenytoin N-demethylation (CYP2B6), paclitaxel 6α-hydroxylation (CYP2C8), Dicrofenac 4'-hydroxylation (CYP2C9), S-mephenytoin 4-hydroxylation (CYP2C19), dextromethorphan O-demethylation (CYP2D6), chlorzoxazone 6-hydroxylation (CYP2E1), testosterone 6β-hydroxylation (CYP3A4/5), and lauric acid 12-hydroxylation (CYP4A). Microsomes were stored at -80°C until use.

Microsomal incubations: P450 mediated metabolic reactions were proceeded at 37°C using a 100 mM potassium phosphate buffer (pH 7.4) and a NADPH generating system which contained final concentrations of 1.25-2.5 mM NADP, 1-10 mM $MgCl_2 \cdot 6H_2O$, 12.5-25 mM glucose-6-phosphate, and 0.5-1 U/mL glucose-6-phosphate dehydrogenase. The rate of formation of the metabolite (V: pmol/min/mg protein or pmol/h/mg protein or pmol/min/pmol CYP) was determined in each experiment.

In the experiments measuring the enzyme kinetic parameters in human hepatic microsomes, final concentrations of 7.8-250 μM pactimibe and 0.78-100 μM R-125528 were incubated for 30 and 15 min, respectively. To determine the enzyme kinetic

parameters for glucuronidation, final concentrations of 50-2000 µM ^{14}C-pactimibe were incubated for 120 min. Due to the absence of an authentic sample of the glucuronide of pactimibe, structure analysis of the metabolite separated by HPLC was conducted by mass spectrometry. Under the conditions used, the formation of the metabolites were linear with respect to incubation time and protein concentrations.

In the experiment of human P450 expressing microsomes, protein concentrations were set at 0.5-1 mg/mL. A hundred mM tris buffer (pH7.4) was used instead of a 100 mM potassium phosphate buffer for the CYP2A6, CYP2C9, and CYP4A11 reactions. Final substrate concentrations and reaction times were set at 7.8-250 µM and 30 min to determine the enzyme kinetic parameters for the formation of M-1 and R-125528 from pactimibe. For the formation of M-2 (the ω-1 oxidized form of R-125528) from R-125528, a metabolic reaction was conducted at a final concentration of 5 µM R-125528 for 15 min.

In correlation experiments, final protein concentrations, substrate concentrations and reaction times were set at 1 mg/mL, 100 µM and 30 min, and 0.5 mg/mL, 10 µM and 15 min when pactimibe and R-125528 were used as substrates, respectively.

The reaction was stopped by the addition of acetonitrile/1N HCl/200 mM dithiothreitol (98:1:1, v/v/v) containing internal standards. The mixture was centrifuged at 15,000 rpm for 3 min at 4°C (himac CF15R, Hitachi Koki, Ltd., Tokyo, Japan). The supernatant fraction was injected into a HPLC or LC-MS/MS system for analysis.

Free fraction of test substance in microsomes: In the experiments measuring the

enzyme kinetic parameters, final concentrations of pactimibe and R-125528 were corrected by multiplying the free fraction percentage of each test substance in the microsomal incubation mixture. Free fraction was experimentally determined by modification in a previously described method (Nakai et al., 2004). In brief, a microsomal incubation mixture without using a NADPH generating system was made. Of the mixture, an aliquot was collected and combined with acetonitrile/1N HCl/200 mM dithiothreitol (98:1:1, v/v/v). The rest of the mixture was ultracentrifuged at 105,000g (Optima^{TM} MAX, Beckman Coulter, Inc., Fullerton, CA) for 30 min at 4°C and an aliquot of the supernatant was collected and combined with acetonitrile/1N HCl/200 mM dithiothreitol (98:1:1, v/v/v). The concentrations of the test substance in pre- and post-ultracentrifugation samples were determined and the ratio of the free form in the sample was calculated by dividing the concentration in the post-ultracentrifugation sample by the concentration in the pre-ultracentrifugation sample.

Analysis

LC-MS/MS method was applied for the measurement of pactimibe, R-125528, and M-1 in an incubation mixture using d_6-M-1 as deuterated internal standards. Separation by HPLC was performed using a Waters Alliance 2795 Separation Module (Waters Corporation, Milford, MA, USA) with a Hydrosphere C_{18} column (150 x 2 mm, 5 μm, YMC Co., Ltd.). The mobile phases were (A) 95% H_2O, 5% acetnitrile, 0.1% formic acid, and 5 mM ammonium acetate and (B) 5% H_2O, 95% acetnitrile, 0.1% formic acid, and 5 mM ammonium acetate. The mobile phase was set at (A)/(B)=33%/67% in an isocratic

mode and the solvent flow rate was 0.2 mL/min. Mass spectra were determined with a

Micromass Quattro LC-MS/MS system (Micromass UK Ltd, Manch, UK). The following

parent and daughter ions (m/z) were monitored: 417.5 and 399.5 for pactimibe, 415.5 and

369.5 for R-125528, 433.5 and 415.4 for M-1, and 439.5 and 421.5 for d_6-M-1,

respectively.

The analysis of M-2 was performed via HPLC using an LC-10AT (Shimadzu

Corporation) as a pump and an SPD-10AV (Shimadzu Corporation) as a detector. A

Symmetry C18 (5 μm, 4.6 mm I.D. × 150 mm, Waters Corporation.) was used for the

column separation. The UV and column temperature were set at 230 nm and 40°C,

respectively. The mobile phases were (A) 50 mM phosphate buffer (pH 2.5) and (B)

acetonitrile and a gradient of [time (min)/% (B): 0 → 8/35 → 70, 8 → 12/70, 12 → 17/35]

was used. The solvent flow rate was set at 1 mL/min.

For the analysis of pactimibe glucuronide, a Symmetry C18 (5 μm, 4.6 mm I.D.

× 150 mm, Waters Corporation.) was used for column separation. The mobile phases

were (A) H_2O containing 0.1% trifluoroacetic acid and (B) acetonitrile containing 0.1%

trifluoroacetic acid. The time programming was as follows: [time (min)/% (B): 0 →

7.5/40 (constant), 7.5 → 8.5/100 (constant), 8.5 → 15/40 (constant). The solvent flow

rate was set at 1 mL/min. The HPLC eluents were collected in scintillation vials with a

fraction collector (L-5200, Hitachi, Ltd.) at 30-sec intervals, and the scintillator

(PICO-FLUOR[TM]40, Packard BioScience, Groningen, Netherlands) was added to each

vial. The radioactivity of the fraction corresponding to pactimibe glucuronide was

measured using a liquid scintillation analyzer (TRI-CARB[®] 2250CA, TRI-CARB[®]

2300TR, Packard BioScience).

Data presentations

Km (µM), Vmax (pmol/min/mg-protein or pmol CYP) and CLint defined as Vmax/Km

(µl/min/mg-protein or pmol CYP) were calculated using WinNonlin (Ver 1.5 or 4.0.1,

Scientific Consulting Inc., Apex, N.C.) and Microsoft Excel (Microsoft Corp., Redwood,

WA) by fitting the data to the following equation: $V = Vmax \times [S]/(Km+[S])$, where V and

[S] represents the initial rate of metabolite formation and free concentration of the test

substance in microsomal incubation mixture, respectively. Correlation coefficients (r^2)

obtained from linear regression analysis were calculated with Microsoft Excel.

Results

Metabolism of pactimibe

The enzyme kinetic parameters for the formation of M-1, R-125528, and glucuronide from pactimibe were determined using pooled human hepatic microsomes. The formation of the N-dealkylated form was not examined due to the low metabolic activity for the reaction in human hepatic microsomes (data not shown). CLint values for the formation of M-1 and R-125528 were almost the same, 0.76 and 0.63 µL/min/mg-protein, respectively (Table 1). The CLint for glucuronide formation from pactimibe was quite low (0.16 µL/min/mg-protein) compared to P450 mediated oxidation.

To elucidate the P450 isoform which is involved in the formation of M-1, microsomes expressing human P450 isoforms were incubated with pactimibe. As shown in Table 2, CYP2C9, CYP2C19, and CYP2D6 showed metabolic activity for M-1 formation. CLint values of CYP2C9, CYP2C19, and CYP2D6 for the formation of M-1 were 0.001, 0.026, and 0.124 µL/min/pmol CYP, respectively. Considering the P450 content (pmol/mg-protein) in human liver microsomes (Rodrigues, 1999), contribution of each P450 isoform involved in the formation of M-1 was calculated to be 5.2, 27, and 67.8%, respectively, suggesting that mainly CYP2D6 contributes to the ω-1 oxidation of pactimibe. As shown in Table 2, P450 expression microsomes revealed that CYP2C19, CYP2D6, and CYP3A4 showed metabolic activity in R-125528 formation. However, CLint values for CYP2C19 and CYP2D6 were quite low (less than 0.002 µL/min/pmol CYP). Considering the high amount of CYP3A4 protein content compared to CYP2C19

13

DMD#18853

and CYP2D6 in human hepatic microsomes, CYP3A4 was estimated to be the major contributor of indolin oxidation in pactimibe.

To obtain further information on P450 isoforms involved in the metabolism of pactimibe, human liver microsomes from 16 different donors, where P450 activities had been known, were incubated. Correlation between the rate of formation of pactimibe metabolites (M-1 and R-125528) and different P450 marker activities are listed in Table 3. The relationship between dextromethorphan O-demethylation activity, a marker for CYP2D6 activity (Schmid et al., 1985), and the rate of M-1 formation was moderately (r^2=0.52) correlated. With regard to the rate of R-125528 formation, testosterone 6β-hydroxylation (r^2=0.86), a marker for CYP3A activity (Waxman et al., 1988) was strongly correlated, whereas no remarkable correlation was observed for other P450 activities. These results support the idea that mainly CYP2D6 and CYP3A4 are involved in the formation of M-1 and R-125528 from pactimibe, respectively.

Metabolism of R-125528

To clarify the elimination pathway of R-125528, the main and only metabolite in systemic circulation, we performed a metabolic study using pooled human hepatic microsomes (Figure 2), microsomes expressing human P450 isoforms (Figure 3A) and a reaction phenotyping kit (Figure 3B). As depicted in Figure 2, enzyme kinetic parameters, Km, Vmax, and Clint values for the ω-1 oxidation of R-125528 (formation of M-2) in pooled human liver microsomes were calculated to be 1.8 µM, 135.0 pmol/min/mg-protein, and 75.0 µl/min/mg-protein, respectively.

14

To elucidate the P450 isoform which is involved in the formation of M-2, microsomes expressing human P450 isoforms were incubated with R-125528. The ω-1 oxidation of R-125528 was observed only in CYP2D6 expressing microsomes (Figure 3A). In addition, the relationship between the rate of ω-1 oxidation of R-125528 and CYP2D6 activity was strongly (r^2=0.90) correlated, suggesting CYP2D6 is highly involved in the metabolism of R-125528 (Figure 3B).

Discussion

A proposed main metabolic pathway of pactimibe in humans is illustrated in Figure 4. Pactimibe has multiple metabolic pathways, that is, oxidation at the indolin ring, ω-1 oxidation at the octyl chain, N-dealkylation and glucuronidation on the carboxylic acid. Metabolic studies using human liver microsomes revealed that indolin ring oxidation (formation of R-125528) and ω-1 oxidation (formation of M-1) were dominant and the CLint values for these metabolisms were 0.63 and 0.76 μl/min/mg-protein, respectively (Table 1). Moreover, according to a P450-isozyme identification study using P450 expression microsomes and a correlation analysis using human liver microsomes, the indolin oxidation and the ω-1 oxidation were found to be catalyzed mainly by CYP3A4 and CYP2D6, respectively (Table 2 and 3).

On the other hand, the metabolic reaction for R-125528 was restricted. Using human hepatic microsomes, R-125528 was only metabolized in the P450 reaction system, but was not conjugated in the UGT reaction system. In rat bile, the only metabolite derived from R-125528 was the ω-1 oxidized form. No glucuronide form was observed (data not shown). In human hepatic microsomes, the CLint value for the formation of M-2, the ω-1 oxidized form of R-125528, was 75.0 μl/min/mg-protein. (Figure 2). P450-isozyme identification study using P450 expression microsomes revealed that CYP2D6 was the only isoform that could catalyze the reaction (Figure 3A). In addition, the reaction phenotyping study indicated CYP2D6 activity was strongly (r^2=0.90) correlated with the formation of M-2 (Figure 3B). Considering that R-125528 itself could not be excreted into the bile nor urine as an intact form, the ω-1 oxidation mediated by

16

DMD#18853

CYP2D6 was considered to be a crucial pathway for the elimination of R-125528 from systemic circulation.

CYP2D6 is one of the best known P450 isoform that leads to large inter-individual variations in drug concentration, drug response, therapeutic outcome and/or toxicity due to its polymorphic nature (Brynne et al., 1998; Molden et al., 2002; Fux et al., 2005). The variability in CYP2D6 activity is mainly genetically determined, and 5% to 10% of Caucasians are reported to express a poor CYP2D6-metabolizing phenotype, resulting from the inheritance of two mutant null alleles (van der Weide and Steijns, 1999). Therefore, it was necessary to examine whether CYP2D6 polymorphism is clinically significant on pharmacokinetic behavior of pactimibe and R-125528 in humans.

It is reported elsewhere (Ito et al., 2005; Gibbs et al., 2006) that AUC increase in CYP2D6 poor metabolizers, is calculated from the following equation (1), $AUC^{PM}/AUC^{EM}=1/(1-fm_{CYP2D6})$. Pactimibe was suggested to have multiple metabolic pathways (i.e. similar contribution of indolin oxidation and ω-1 oxidation besides glucuronidation to some extent, Table 1). Assuming that fm_{CYP2D6} (fraction of metabolism via CYP2D6) of pactimibe is estimated to be 0.5 at most, AUC increase of pactimibe in CYP2D6 poor metabolizers is expected to be within 2-fold. Similarly, even if the CYP3A4 mediated pathway is completely abolished by concomitant use of strong CYP3A4 inhibitors such as ketoconazole, AUC increase of pactimibe would be within 2-fold. It can be said that the multiple metabolic pathway of pactimibe will minimize the extent of drug-drug interaction and/or the effect of genetic polymorphisms.

17

On the other hand, based on equation (1), due to the nonlinear shape of the relationship between fm_{CYP2D6} and AUC^{PM}/AUC^{EM}, small changes in percentage contribution can result in large pharmacokinetic differences when the fraction metabolized exceeds 60% (Gibbs et al., 2006). Therefore, the effect of CYP2D6 polymorphism on pharmacokinetics of R-125528 is expected to be more severe than that of pactimibe.

Even though R-125528 is pharmacologically inactive, to monitor the plasma concentration level of this metabolite in humans will be of great importance from toxicological point of view. Metabolite safety testing has also been recommended in the Food and Drug Administration guide for industries (CDER, 2005). The guidance stated that major human metabolites should be monitored in clinical trials and that exposure to subjects should be guaranteed by non-clinical safety studies within an adequate margin.

In the case of pactimibe, when CYP2D6 activity is decreased, the exposure of R-125528 could be drastically increased due to its considerably high fm_{CYP2D6}. The idea reminded us of the concern that the exposure of R-125528 after multiple doses of pactimibe sulfate in CYP2D6 poor metabolizers might exceed the animal NOAEL (No Observed Adverse Effect Level). If changes in the pharmacokinetics have a significant impact on both the safety and pharmacological activity of this compound, dose adjustment in CYP2D6 poor metabolizers and/or exclusion of CYP2D6 poor metabolizers may be necessary in clinical settings.

To assess the safety of this compound in humans, the following have been suggested to conduct during development: 1) drug-drug interaction studies with CYP2D6

18

inhibitors, 2) confirmation of the exposure and safety levels of pactimibe and R-125528

in CYP2D6 poor metabolizers after single dose administration and simulating exposure

levels after multiple dose in CYP2D6 poor metabolizers, 3) confirmation of the exposure

and safety of pactimibe and R-125528 in CYP2D6 poor metabolizers after multiple dose

administration.

Several efforts have been directed for predicting binding affinity against

CYP2D6 using in silico methods (Strobl et al., 1993; de Groot et al., 1999a, 1999b; Ekins

et al., 2003). Ellis *et al*. (Ellis et al., 1995) demonstrated that Asp^{301} plays an important

role in determining the substrate specificity and activity of CYP2D6 and provided

experimental evidence for the electrostatic interaction between the basic nitrogen in

CYP2D6 substrates and the carboxylate group of Asp^{301}. Paine *et al*. (Paine et al., 2003)

also suggested the importance of Glu^{216} in addition to Asp^{301} as key determinant factors

for substrate specificity and product regioselectivity in CYP2D6. Therefore, it has been

recognized that the presence of basic nitrogen is essential for CYP2D6 substrates to

interact with the carboxylate anion of Asp^{301} or Glu^{216}.

In this study, we found that both pactimibe and R-125528 are CYP2D6

substrates, and to our surprise that R-125528 is an especially good and specific substrate

for CYP2D6. The Km value was 1.8 μM for CYP2D6 mediated ω-1 oxidation of

R-125528 in human hepatic microsomes, indicating very high affinity for CYP2D6 of

this acidic compound. Although R-125528 has a nitrogen atom in the indole ring, it is not

protonated in the whole pH range. Thus, R-125528 is thought to be a very unique

CYP2D6 substrate devoid of basic nitrogen. Recently, Guengerich *et al*. (Guengerich et

al., 2002) also identified a ligand, spirosulfonamide, devoid of basic nitrogen but having a high affinity for CYP2D6.

In conclusion, we conducted metabolic studies of pactimibe and its plasma metabolite, R-125528. We found that R-125528 needs to be metabolized solely by CYP2D6 to be eliminated, suggesting several studies with CYP2D6 including drug-drug interaction and polymorphism sensitivity should be conducted during clinical development from the viewpoint of metabolite safety assessment. The finding that R-125528, an acidic compound devoid of basic nitrogen, was a good substrate for CYP2D6 raises questions about the previously reported CYP2D6 models based on a critical electrostatic interaction with Asp^{301} and/or Glu^{216}.

References

Brynne N, Dalen P, Alvan G, Bertilsson L and Gabrielsson J (1998) Influence of
CYP2D6 polymorphism on the pharmacokinetics and pharmacodynamic of
tolterodine. *Clin Pharmacol Ther* 63:529-539.

CDER (2005) Guidance for industry –Safety testing of drug metabolites-, Center for
Drug Evaluation and Research at Food and Drug Administraion.

de Groot MJ, Ackland MJ, Horne VA, Alex AA and Jones BC (1999a) Novel approach to
predicting P450-mediated drug metabolism: development of a combined protein
and pharmacophore model for CYP2D6. *J Med Chem* 42:1515-1524.

de Groot MJ, Ackland MJ, Horne VA, Alex AA and Jones BC (1999b) A novel approach
to predicting P450 mediated drug metabolism. CYP2D6 catalyzed N-dealkylation
reactions and qualitative metabolite predictions using a combined protein and
pharmacophore model for CYP2D6. *J Med Chem* 42:4062-4070.

Ekins S, Berbaum J and Harrison RK (2003) Generation and validation of rapid
computational filters for cyp2d6 and cyp3a4. *Drug Metab Dispos* 31:1077-1080.

Ellis SW, Hayhurst GP, Smith G, Lightfoot T, Wong MM, Simula AP, Ackland MJ,
Sternberg MJ, Lennard MS, Tucker GT and et al. (1995) Evidence that aspartic
acid 301 is a critical substrate-contact residue in the active site of cytochrome
P450 2D6. *J Biol Chem* 270:29055-29058.

Fux R, Morike K, Prohmer AM, Delabar U, Schwab M, Schaeffeler E, Lorenz G, Gleiter
CH, Eichelbaum M and Kivisto KT (2005) Impact of CYP2D6 genotype on
adverse effects during treatment with metoprolol: a prospective clinical study.

Clin Pharmacol Ther 78:378-387.

Gibbs JP, Hyland R and Youdim K (2006) Minimizing polymorphic metabolism in drug

discovery: evaluation of the utility of in vitro methods for predicting

pharmacokinetic consequences associated with CYP2D6 metabolism. *Drug*

Metab Dispos 34:1516-1522.

Guengerich FP, Miller GP, Hanna IH, Martin MV, Leger S, Black C, Chauret N, Silva JM,

Trimble LA, Yergey JA and Nicoll-Griffith DA (2002) Diversity in the oxidation

of substrates by cytochrome P450 2D6: lack of an obligatory role of aspartate

301-substrate electrostatic bonding. *Biochemistry* 41:11025-11034.

Hainer JW, Terry JG, Connell JM, Zyruk H, Jenkins RM, Shand DL, Gillies PJ, Livak KJ,

Hunt TL and Crouse JR, 3rd (1994) Effect of the acyl-CoA:cholesterol

acyltransferase inhibitor DuP 128 on cholesterol absorption and serum cholesterol

in humans. *Clin Pharmacol Ther* 56:65-74.

Harris WS, Dujovne CA, von Bergmann K, Neal J, Akester J, Windsor SL, Greene D and

Look Z (1990) Effects of the ACAT inhibitor CL 277,082 on cholesterol

metabolism in humans. *Clin Pharmacol Ther* 48:189-194.

Ishi M, Tomono Y, Sanma H, Yamoto C, Sekino H, Nomura M and Nakaya N (1994)

Pharmacokinetics of novel ACAT inhibitor E5324, in healthy volunteers.

Atheroscrelosis 109:283 (253-Abs).

Ito K, Hallifax D, Obach RS and Houston JB (2005) Impact of parallel pathways of drug

elimination and multiple cytochrome P450 involvement on drug-drug

interactions: CYP2D6 paradigm. *Drug Metab Dispos* 33:837-844.

Kashiwa M, Masuyama Y, Miyauchi H, Uchida T, Naganuma S, Kakuta H, Terada M, Kiriyama T, Matsuda K, Ito N, Iizumi Y and Takenaka T (1997) Pharmacological properties of YM17E, an acyl-CoA:cholesterol acyltransferase inhibitor, and diarrheal effect in beagle dogs. *Jpn J Pharmacol* 73:41-50.

Kitayama K, Koga T, Inaba T and Fujioka T (2006a) Multiple mechanisms of hypocholesterolemic action of pactimibe, a novel acyl-coenzyme A:cholesterol acyltransferase inhibitor. *Eur J Pharmacol* 543:123-132.

Kitayama K, Koga T, Maeda N, Inaba T and Fujioka T (2006b) Pactimibe stabilizes atherosclerotic plaque through macrophage acyl-CoA:cholesterol acyltransferase inhibition in WHHL rabbits. *Eur J Pharmacol* 539:81-88.

Kitayama K, Tanimoto T, Koga T, Terasaka N, Fujioka T and Inaba T (2006c) Importance of acyl-coenzyme A:cholesterol acyltransferase 1/2 dual inhibition for anti-atherosclerotic potency of pactimibe. *Eur J Pharmacol* 540:121-130.

Matsuo M, Hashimoto M, Suzuki J, Iwanami K, Tomoi M and Shimomura K (1996) Difference between normal and WHHL rabbits in susceptibility to the adrenal toxicity of an acyl-CoA:cholesterol acyltransferase inhibitor, FR145237. *Toxicol Appl Pharmacol* 140:387-392.

Molden E, Johansen PW, Boe GH, Bergan S, Christensen H, Rugstad HE, Rootwelt H, Reubsaet L and Lehne G (2002) Pharmacokinetics of diltiazem and its metabolites in relation to CYP2D6 genotype. *Clin Pharmacol Ther* 72:333-342.

Nakai D, Kumamoto K, Sakikawa C, Kosaka T and Tokui T (2004) Evaluation of the protein binding ratio of drugs by a micro-scale ultracentrifugation method. *J*

Pharm Sci 93:847-854.

Nakaya N, Nakamichi N, Sekino H, Nomura M, Ishii M, Tomono Y and Yamato C
(1994) Effect of a novel ACAT inhibitor, E5324, on serum lipids and lipoproteins
in healthy volunteers, in: *Atheroscrelosis*, pp 284 (253-Abs).

Nissen SE, Tuzcu EM, Brewer HB, Sipahi I, Nicholls SJ, Ganz P, Schoenhagen P, Waters
DD, Pepine CJ, Crowe TD, Davidson MH, Deanfield JE, Wisniewski LM,
Hanyok JJ and Kassalow LM (2006) Effect of ACAT inhibition on the
progression of coronary atherosclerosis. *N Engl J Med* 354:1253-1263.

Paine MJ, McLaughlin LA, Flanagan JU, Kemp CA, Sutcliffe MJ, Roberts GC and Wolf
CR (2003) Residues glutamate 216 and aspartate 301 are key determinants of
substrate specificity and product regioselectivity in cytochrome P450 2D6. *J Biol
Chem* 278:4021-4027.

Peck RW, Wiggs R and Posner J (1995) The tolerability, pharmacokinetics and lack of
effect on plasma cholesterol of 447C88, an AcylCoA: Cholesterol Acyl
Transferase (ACAT) inhibitor with low bioavailability, in healthy volunteers. *Eur
J Clin Pharmacol* 49:243-249.

Reindel JF, Dominick MA, Bocan TM, Gough AW and McGuire EJ (1994) Toxicologic
effects of a novel acyl-CoA:cholesterol acyltransferase inhibitor in cynomolgus
monkeys. *Toxicol Pathol* 22:510-518.

Rodrigues AD (1999) Integrated cytochrome P450 reaction phenotyping: attempting to
bridge the gap between cDNA-expressed cytochromes P450 and native human
liver microsomes. *Biochem Pharmacol* 57:465-480.

Schmid B, Bircher J, Preisig R and Kupfer A (1985) Polymorphic dextromethorphan metabolism: co-segregation of oxidative O-demethylation with debrisoquin hydroxylation. *Clin Pharmacol Ther* 38:618-624.

Strobl GR, von Kruedener S, Stockigt J, Guengerich FP and Wolff T (1993) Development of a pharmacophore for inhibition of human liver cytochrome P-450 2D6: molecular modeling and inhibition studies. *J Med Chem* 36:1136-1145.

Tardif JC, Gregoire J, L'Allier PL, Anderson TJ, Bertrand O, Reeves F, Title LM, Alfonso F, Schampaert E, Hassan A, McLain R, Pressler ML, Ibrahim R, Lesperance J, Blue J, Heinonen T and Rodes-Cabau J (2004) Effects of the acyl coenzyme A:cholesterol acyltransferase inhibitor avasimibe on human atherosclerotic lesions. *Circulation* 110:3372-3377.

Terasaka N, Miyazaki A, Kasanuki N, Ito K, Ubukata N, Koieyama T, Kitayama K, Tanimoto T, Maeda N and Inaba T (2007) ACAT inhibitor pactimibe sulfate (CS-505) reduces and stabilizes atherosclerotic lesions by cholesterol-lowering and direct effects in apolipoprotein E-deficient mice. *Atherosclerosis* 190:239-247.

van der Weide J and Steijns LS (1999) Cytochrome P450 enzyme system: genetic polymorphisms and impact on clinical pharmacology. *Ann Clin Biochem* 36 (Pt 6):722-729.

Venkatakrishnan K, Von Moltke LL and Greenblatt DJ (2001) Human drug metabolism and the cytochromes P450: application and relevance of in vitro models. *J Clin*

Pharmacol 41:1149-1179.

Vernetti LA, MacDonald JR, Wolfgang GH, Dominick MA and Pegg DG (1993) ATP

depletion is associated with cytotoxicity of a novel lipid regulator in guinea pig

adrenocortical cells. *Toxicol Appl Pharmacol* 118:30-38.

Waxman DJ, Attisano C, Guengerich FP and Lapenson DP (1988) Human liver

microsomal steroid metabolism: identification of the major microsomal steroid

hormone 6 beta-hydroxylase cytochrome P-450 enzyme. *Arch Biochem Biophys*

263:424-436.

Legends for figures

Figure 1.   Chemical structure of pactimibe sulfate

Figure 2.   [S]-V plots for the formation of M-2 from R-125528 in pooled human microsomes. ([S]; free concentration of R-125528, V; formation rate of M-2). Final concentrations of 0.78-100 μM R-125528 were incubated for 15 min. The solid line represents the best-fit line by fitting the data to the equation described in Material and Methods.

Figure 3.   (A) The formation of M-2 from R-125528 in microsomes expressing human P450 isoforms. Final concentration of 5 μM R-125528 was incubated for 15 min. N.D., Not detectable. (B) Relationships between dextromethorphan O-demethylation activity, a marker for CYP2D6 activity and the formation of M-2 from R-125528 in human hepatic microsomes (N=16). Final protein concentration, substrate concentration and reaction time were set at 0.5 mg/mL, 10 μM and 15 min, respectively. The solid line represents the least-squares fit from linear regression analysis. Correlation coefficients were calculated with Microsoft Excel 97.

Figure 4.   Proposed main metabolic pathway of pactimibe in human

Table 1. Enzyme kinetic parameters for the formation of M-1 and R-125528, and glucuronide form from pactimibe in pooled human liver microsomes

Metabolism	Km	Vmax	CLint
	(μM)	(pmol/min/mg-protein)	(μl/min/mg-protein)
M-1 formation	90.5	68.8	0.76
R-125528 formation	107.2	67.8	0.63
Glucuronide formation	299.6	47.5	0.16

For M-1 and R-125528 formation, final concentrations of 7.8-250 μM pactimibe were incubated for 30 and 15 min, respectively. For glucuronide formation, final concentrations of 50-2000 μM ^{14}C-pactimibe were incubated for 120 min.

Table 2. Enzyme kinetic parameters and estimated contribution ratio for each P450 isoform involved in the formation of M-1 and R-125528

Metabolism	P450 isoform	Km (µM)	Vmax (pmol/min/pmol CYP)	CLint (µL/min/pmol CYP)	Contents[a] (pmol/mg P)	%contribution[b] (%)
	CYP2C9	123.1	0.16	0.001	96	5.2
M-1 formation	CYP2C19	210.2	5.5	0.026	19	27
	CYP2D6	25.1	3.1	0.124	10	67.8
	CYP2C19	869.3	0.72	0.001	19	0.5
R-125528 formation	CYP2D6	683.4	1.1	0.002	10	0.5
	CYP3A4	26.8	1.0	0.037	108	99

For M-1 and R-125528 formation, final concentrations of 7.8-250 µM pactimibe were

incubated for 30 min.

a Rodrigues AD (1999)

b Calculated from CLint for each P450 isoform and P450 content

Table 3.   Correlation between the formation rate of pactimibe metabolites and different

P450 marker activities in human hepatic microsomes (N =16)

P450 isofroms	Marker reaction	Correlation (r^2)	
		M-1 formation	R-125528 formation
CYP 1A2	7-ethoxyresorufin O-dealkylation	0.019	0.025
CYP 2A6	Coumarin 7-hydroxylation	0.0018	0.01
CYP 2B6	S-Mephenytoin N-demethylation	0.25	0.23
CYP 2C8	Paclitaxel 6α-hydroxylation	0.54	0.45
CYP 2C9	Dicrofenac 4'-hydroxylation	0.18	0.065
CYP 2C19	S-Mephenytoin 4'-hydroxylation	0.18	0.08
CYP2D6	Dextromethorphan O-demethylation	0.52	0.022
CYP2E1	Chlorzoxazone 6-hydroxylation	0.015	0.0022
CYP3A4/5	Testosterone 6β-hydroxylation	0.27	0.86
CYP4A9/11	Lauric acid 12-hydroxylation	0.04	0.062

Final protein concentration, substrate concentration and reaction time were set at 1

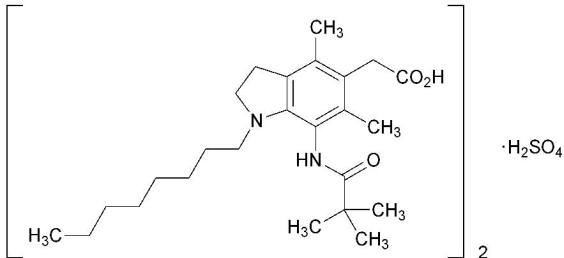mg/mL, 100 μM and 30 min, respectively.
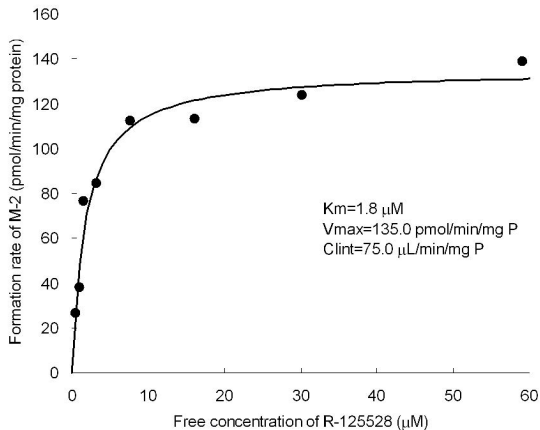
Figure 1.

Figure 2.

Km=1.8 μM
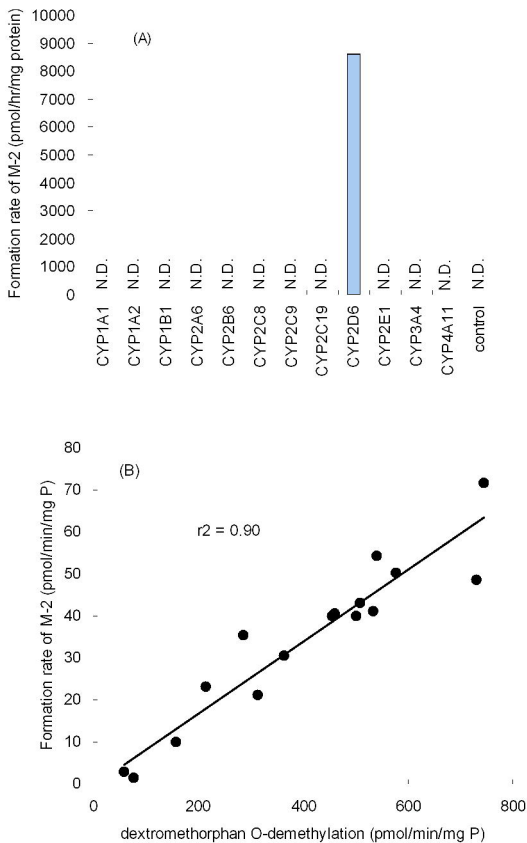Vmax=135.0 pmol/min/mg P
Clint=75.0 μL/min/mg P

Figure 3.

Figure 4.

Glucuronidation

N-dealkylation

Pactimibe

CYP2D6 M-1

CYP3A4

R-125528

CYP2D6 M-2